Solid Freeform Fabrication 2019: Proceedings of the 30th Annual International Solid Freeform Fabrication Symposium – An Additive Manufacturing Conference
Reviewed Paper

VERY HIGH CYCLE FATIGUE BEHAVIOR OF LASER BEAM-POWDER BED FUSED INCONEL 718

Palmer Frye[1], Muztahid Muhammad[2,3], Jutima Simsiriwong[1]*, and Nima Shamsaei[2,3]

[1]School of Engineering, University of North Florida, Jacksonville, FL 32224
[2]Department of Mechanical Engineering, Auburn University, Auburn, AL 36849
[3]National Center for Additive Manufacturing Excellence (NCAME), Auburn University, Auburn, AL 36849

*Corresponding author:
Email: j.simsiriwong@unf.edu
Phone: (904)620-5351

Abstract

In this study, the very high cycle fatigue (VHCF) behavior of Inconel 718 manufactured via a Laser Beam-Powder Bed Fusion (LB-PBF) process is investigated. LB-PBF Inconel 718 specimens are fabricated in vertical direction and subjected to post-processing heat treatment. The experiment is conducted on as built (i.e. non-machined) specimens utilizing an ultrasonic fatigue test system operating at 20 kHz under force-controlled fully-reversed constant amplitude cyclic loading. Fractography analysis is performed using a digital microscope to identify microstructural features that initiate fatigue cracks in the specimens. Experimental results from LB-PBF Inconel 718 specimens are presented and compared to those of wrought Inconel 718. It is determined that the fatigue resistance of as-built LB-PBF Inconel 718 specimens is significantly less than that of the wrought material. This result is attributed to a large presence of LB-PBF process intrinsic defects. In the VHCF regime, subsurface crack initiation is the primary fatigue failure mechanism in as-built LB-PBF Inconel 718 specimens.

Introduction

Additive manufacturing (AM) of metals has recently been of great interest to aerospace industries due to its significant potential to replace conventional manufacturing methods as a means of full-scale production. Despite the fact of its increased popularity, AM metals have not been adequately characterized and tested for reliability as structural components. In order for AM to surpass the current manufacturing methods, the mechanical behavior under cyclic loading (i.e. fatigue behavior) of AM metals must be fully understood.

Nickel-based super alloys are typically used in applications that require creep rupture resistance, oxidation resistance, and corrosion resistance over a wide temperature range [1]. Turbine blades in jet engines are perhaps the most common application that utilizes these alloys, particularly Inconel 718. In aerospace engines, combustion temperatures could exceed 1,000 °C; therefore, the material of choice for critical engine components must withstand high temperatures while maintaining its mechanical performance especially under realistic cyclic loadings [1]. In addition, aircraft engine components typically require a long service life (>15,000 hours of use) before they are replaced or refurbished [2].

Since critical aerospace engine components must withstand long service lives at high loading frequencies, the understanding of very high cycle fatigue (VHCF) behavior (i.e. cyclic loading beyond 10^7 cycles) of Inconel 718 must be obtained [3]. However, a comprehensive VHCF study is typically considered to be an expensive task from time and cost perspectives [3]. Nonetheless, many researchers have successfully utilized various technique to conduct fatigue testing at VHCF regime by means of ultrasonic fatigue test systems that can simulate fully-reversed (R=-1) cyclic loading at much higher frequencies as compared to the conventional hydraulic fatigue testing [3-6].

Based on various studies on both high cycle fatigue (HCF) and VHCF regimes, fatigue cracks in wrought Inconel 718 tend to initiate from sub-surface locations such as microstructural discontinuities and inclusions [4, 6-8]. Sub-surface fatigue cracks have been found to initiate from two main sources, including carbides (i.e. discontinuities in the microstructure) and large austenite grains [7]. Crack initiation from carbides takes place in the early stages of fatigue due to the brittle nature of carbides. Large presence of carbides within the microstructure of Inconel 718 parts can significantly reduce fatigue strength. Moreover, fatigue cracks initiating in large austenite grains can be identified by the presence of persistent slip bands between grain boundaries [7]. A fatigue strength correlation between austenite grain size and carbide population also exists. Fine grained Inconel parts are much more sensitive to crack initiation when carbides are present [7]. In addition, twin boundaries are also sensitive to crack initiation, especially if carbide population is negligible [7].

AM parts typically contain a variety of process induced defects that are known to be detrimental to fatigue resistance. These defects include entrapped gas pores, lack of fusion defects between build layers, and rough surfaces covered in unmelted powder particles. Many studies have shown that internal defects or discontinuities in the microstructure are the most notable causes of fatigue crack initiation in the VHCF regime [4, 5, 9-14]. However, post-process heat treatment and hot isostatic pressing (HIP) have been shown to reduce the remnant porosity and consequently improve fatigue performance of AM metals [5, 12, 15].

The Laser Beam-Powder Bed Fusion (LB-PBF) process builds parts layer-by-layer, which produces sharp stair-step notches on part surfaces due to 3-D contouring [10]. Additionally, LB-PBF part surfaces contain unmelted metallic powder particles. Surface quality and build direction are known to affect the mechanical properties of AM metallic parts [10]. A relationship between surface finish characteristics of AM Inconel 718 and their influence on VHCF behavior has not be directly investigated. Gunther et al. [12] investigated the effects of surface roughness on high cycle fatigue behavior of AM Ti-6Al-4V through internal channels built into the fatigue specimens. The fractography analysis of this experiment showed that large clusters of unmelted powder of the internal channels were the most common sights for crack initiation [12]. However, this study did highlight the strong influence of internal defects on fatigue crack initiation. It has been proposed that fatigue failure in the VHCF regime uniquely originates from sub-surface defects, but with the lack of knowledge of as-built surface roughness effects on VHCF behavior, it is still an important design consideration that should be further studied.

The aim of this study is to determine the influence of surface quality on the VHCF behavior of AM Inconel 718. Fatigue performance of AM Inconel 718 is compared to its wrought counterpart. This paper first discusses the material of choice for experimentation and experimental methods. Lastly, results and discussion of the results are presented.

Material and Experimental Methods

Wrought and AM Inconel 718 VHCF specimens were fabricated following the geometry shown in Figure 1. Wrought specimens were fabricated from 0.625-inch round bar stock and machined using a Haas ST-20 CNC lathe. The wrought Inconel bar was processed and heat treated to achieve the AMS 5562N and ASTM B637 standards before machining; therefore, no additional heat treatments were applied to the wrought Inconel 718 specimens. Following machining, all wrought test samples were polished using 400 grit, 800 grit, 1000 grit, 1500 grit, and 2000 grit silicon carbide polishing cloths. After preliminary surface treatment with sanding papers, all specimens were polished using a buffing pad and a 6 micron aluminum oxide lapping film.

LB-PBF specimens were manufactured using an EOS M290 Direct Metal Laser Sintering System at the National Center for Additive Manufacturing Excellence at Auburn University. These specimens were heat treated to the same standard specifications as the wrought specimens in this study. The AMS 5562N standard is for solution heat treatment of Inconel 718 bars, sheets, and forgings. The specimens were first held at at a solution set temperature of 954 °C for 10 minutes. They were subsequently transferred to a 718 °C furnace for 8 hours, and 621 °C for a total precipitation time of 18 hours [17]. An image of wrought specimen and an as-built (i.e. non-machined surface condition) LB-PBF specimen can be seen in Figure 2.

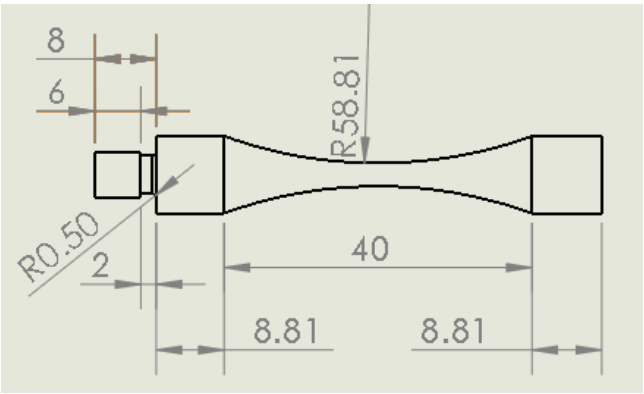

Figure 1. Inconel 718 VHCF specimen geometry (all dimensions are in mm)

Figure 2. (a) wrought-machined and (b) as-built LB-PBF Inconel 718 VHCF test specimens

VHCF testing was conducted under force-controlled, fully-reversed loading at 20 kHz at room temperature and relative humidity. The Shimadzu USF-2000A ultrasonic fatigue test system equipped with a non-contact eddy current extensometer was used in this study. Figure 3 shows the functional principle of the ultrasonic fatigue tester setup. In an ultrasonic fatigue test system, a piezo actuator oscillates at a frequency of 20 kHz, which sends stationary longitudinal waves through the horn and test specimen allowing the test specimen to resonate. The dimensions and geometry of the specimen are designed so that the maximum stress is applied to the gauge section only, and the maximum displacement occurs at the free end and the clamped ends of the specimen. This system allows for simulation of fatigue loading at much higher frequencies as compared to pre-existing fatigue testing machines.

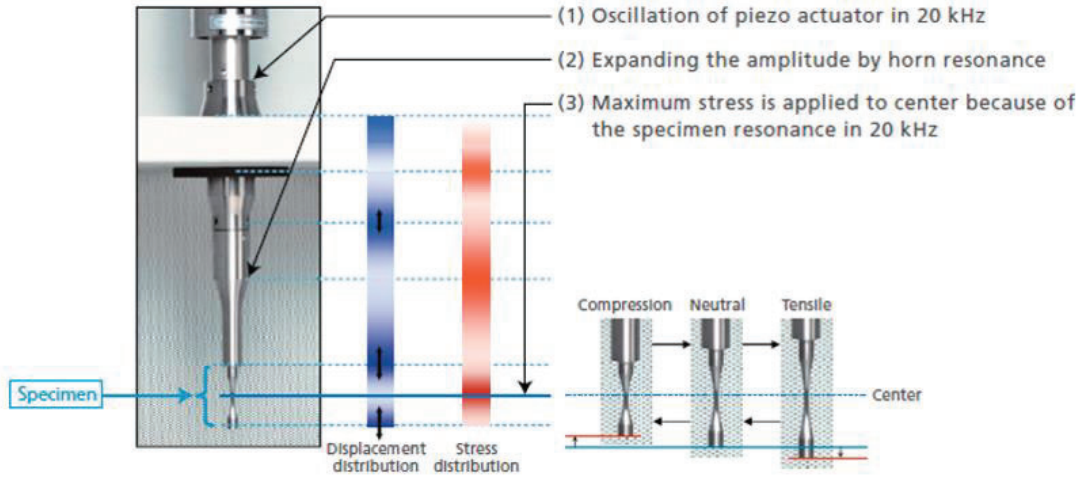

Figure 3. Functional principle of ultrasonic fatigue testing with Shimadzu USF-2000A [18]

Figure 4 depicts the USF-2000A setup used for this experimentation. During testing, the test specimen temperature was closely monitored using a laser thermometer. The temperature rise of the specimen was kept less than 30 °C to minimize the effects of thermal expansion. Temperature rise was also minimized using coolant (air) flow directly to the gauge section of the test specimen, as well as intermittent driving pulse/pause conditions to negate thermal expansion effects from self-heating. Intermittent pulse/pause parameters varied from 110/800 msec to 110/4000 milliseconds, depending on the stress amplitude. A calibration of the extensometer and piezo-electric transducer were carried out prior to testing based on the standard operating procedure provided by the manufacturer of the test system. Each test is terminated when the observed change in resonance frequency of the test sample exceeds 500 Hz. The predetermined run-out fatigue life was set to 10^9 cycles.

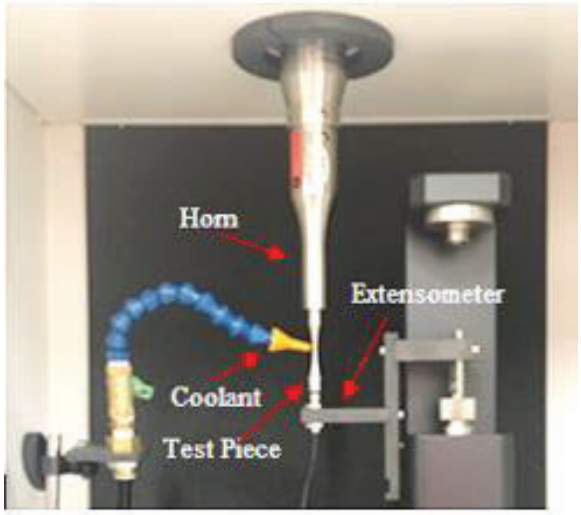

Figure 4. VHCF test setup

A Keyence VHX-6000 digital microscope was used in 3-D depth and composition mode for fracture surface topographical observations. Features including topography, fatigue striations, crack nucleation, and crack propagation regions were identified. The purpose of this study is to analyze the effects of as-built surface quality and intrinsic defects on fatigue crack initiation and fatigue performance of LB-PBF Inconel 718 specimens. LB-PBF Inconel 718 specimens were built to near net-shape specimens and tested in the as-built condition, meaning that no efforts were taken to improve the surface quality of the specimens.

Experimental Results

Figure 5 presents the stress-life data for wrought and LB-PBF Inconel 718 specimens. Runout tests are indicated with an arrow as shown in this figure. It is observed that LB-PBF Inconel 718 specimens exhibit fatigue lives that are at least three orders of magnitude shorter than their wrought counterparts for any given test stress amplitude.

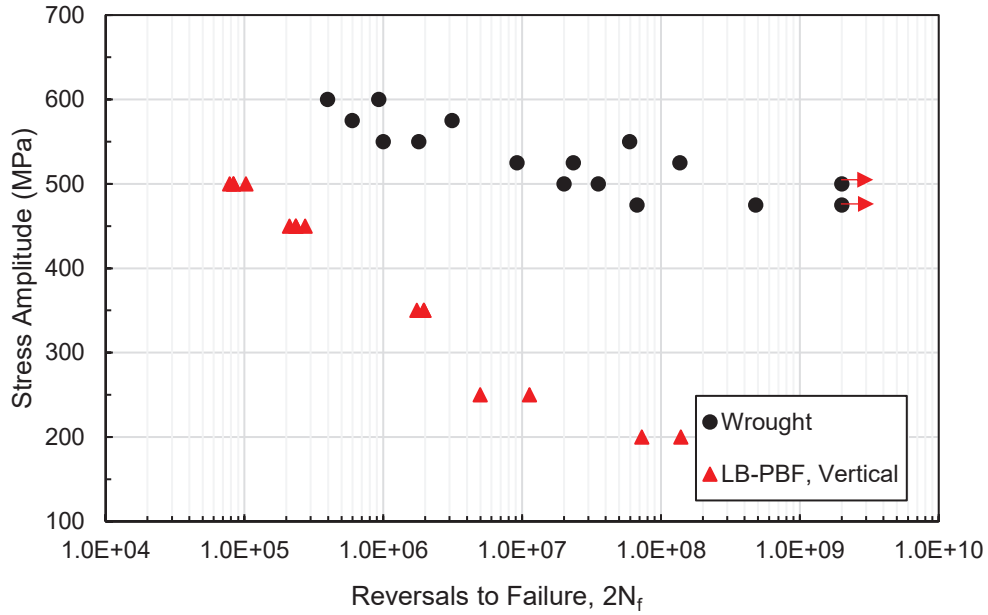

Figure 5. Stress amplitude versus fatigue life data obtained from ultrasonic fatigue tests of vertical as-built LB-PBF and wrought Inconel 718

Fatigue fracture surfaces were investigated using a digital microscope. Figures 6(a) and 6(b) show a fracture surface of the specimen subjected to 350 MPa. For this specimen, the fatigue crack initiated at or just below specimen surfaces at an apparent layer of unmelted powder particles. Figure 6(a) displays the overall fracture surface and Figure 6b is magnified to show the areas of crack growth on the fracture surface.

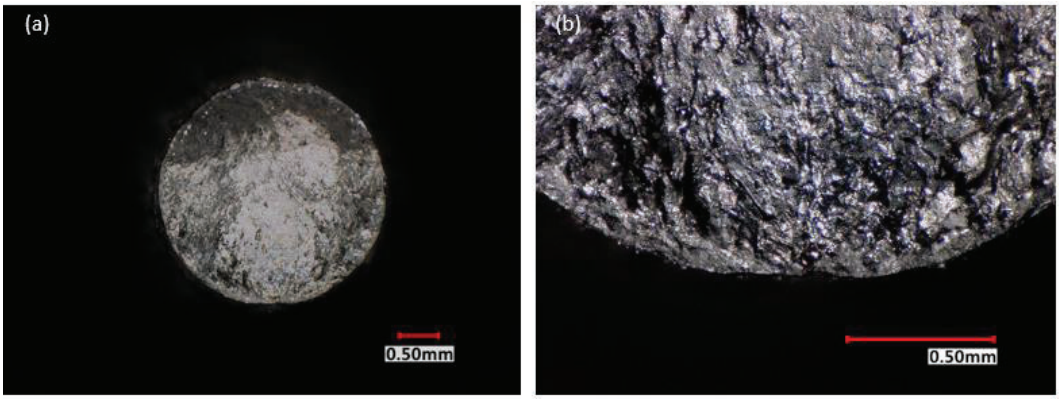

Figure 6. Fatigue fracture surface of as-built LB-PBF specimen (σ_a = 350 MPa and N_f = 9.77E05 cycles) at (a) 20x and (b) 200x magnification

The aim of this experimentation was to test specimens beyond the traditional fatigue limit of 10^7 cycles. However, only two tests at a stress amplitude of 200 MPa were able to exceed the 10^7 cycle threshold. This is due to the limitations imposed by the specimen geometry and the testing equipment available. Based on the specimen geometry and material properties, the ultrasonic fatigue test system was only able to produce a minimum stress amplitude of 200 MPa.

Two tests were run at a stress amplitude of 200 MPa, in which the fracture surface of one of these specimens is shown in Figure 7. Based on the literature [4-6, 14, 16], fatigue cracks in the VHCF regime are expected to initiate below the specimen surface. Similar observation was obtained for the two samples that failed past 10^7 cycles in this study. The overall fracture surface of one of these two samples is shown in Figure 7(a), and the crack initiation region is shown in Figure 7(b).

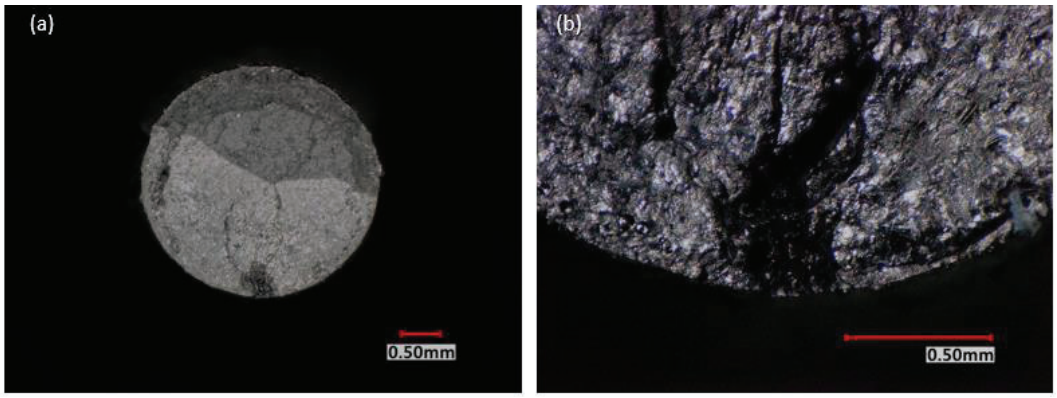

Figure 7. Fatigue fracture surface of as-built LB-PBF specimen (σ_a = 200 MPa and N_f = 3.63E07 cycles) at (a) 20x and (b) 200x magnification

Conclusions

The present study investigated the very high cycle fatigue behavior of as-built LB-PBF manufactured Inconel 718. LB-PBF specimens were subjected to post-processing heat treatment identical to the same specification of the as-received wrought material. The fatigue behavior for as-built LB-PBF and wrought Inconel 718 specimens was compared. The fatigue crack initiation mechanisms were investigated for all as-built LB-PBF specimens. The findings can be summarized as:

- Fatigue resistance of as-built LB-PBF Inconel 718 specimens is significantly less (approximately three orders of magnitude for all test stress amplitudes) than those of wrought counterpart.
- As-built LB-PBF Inconel 718 specimens under cyclic loading experience fatigue failure due to surface crack initiation. Once fatigue life exceeds 10^7 cycles, the primary fatigue failure mode becomes sub-surface crack initiation.

References

[1] Trosch, T., Strößner, J., Völkl, R., & Glatzel, U. (2016). Microstructure and mechanical properties of selective laser melted Inconel 718 compared to forging and casting. *Materials Letters,164*, 428-431.

[2] Retrieved from https://www.faa.gov/documentLibrary/media/Advisory_Circular/AC_120-113.pdf

[3] Bathias, C., & Paris, P. C. (2005). *Gigacycle fatigue in mechanical practice*. New York: Marcel Dekker.

[4] Texier, D., Cormier, J., Villechaise, P., Stinville, J., Torbet, C. J., Pierret, S., & Pollock, T. M. (2016). Crack initiation sensitivity of wrought direct aged alloy 718 in the very high cycle fatigue regime: The role of non-metallic inclusions. *Materials Science and Engineering: A,678*, 122-136.

[5] Günther, J., Krewerth, D., Lippmann, T., Leuders, S., Tröster, T., Weidner, A., Biermann, H., Niendorf, T. (2017). Fatigue life of additively manufactured Ti–6Al–4V in the very high cycle fatigue regime. *International Journal of Fatigue,94*, 236-245.

[6] Chen, Q., Kawagoishi, N., Wang, Q., Yan, N., Ono, T., & Hashiguchi, G. (2005). Small crack behavior and fracture of nickel-based superalloy under ultrasonic fatigue. *International Journal of Fatigue,27*(10-12), 1227-1232.

[7] Klotz, T., Miao, H., Bianchetti, C., Lévesque, M., & Brochu, M. (2018). Analytical fatigue life prediction of shot peened Inconel 718. *International Journal of Fatigue,113*, 204-221.

[8] Kolyshkin, A., Zimmermann, M., Kaufmann, E., & Christ, H. (2016). Experimental investigation and analytical description of the damage evolution in a Ni-based superalloy beyond 106 loading cycles. *International Journal of Fatigue,93*, 272-280.

[9] Seifi, M., Salem, A., Satko, D., Shaffer, J., & Lewandowski, J. J. (2017). Defect distribution and microstructure heterogeneity effects on fracture resistance and fatigue behavior of EBM Ti–6Al–4V. *International Journal of Fatigue,94*, 263-287

[10] Chen, Z., Wu, X., Tomus, D., & Davies, C. H. (2018). Surface roughness of Selective Laser Melted Ti-6Al-4V alloy components. *Additive Manufacturing,21*, 91-103.

[11] Moussaoui, K., Rubio, W., Mousseigne, M., Sultan, T., & Rezai, F. (2018). Effects of Selective Laser Melting additive manufacturing parameters of Inconel 718 on porosity, microstructure and mechanical properties. *Materials Science and Engineering: A,735*, 182-190.

[12] Günther, J., Leuders, S., Koppa, P., Tröster, T., Henkel, S., Biermann, H., & Niendorf, T. (2018). On the effect of internal channels and surface roughness on the high-cycle fatigue performance of Ti-6Al-4V processed by SLM. *Materials & Design,143*, 1-11.

[13] Gopikrishna, D., Jha, S., & Dash, L. (1997). Influence of Microstructure on Fatigue Properties of Alloy 718. *Superalloys 718, 625, 706 and Various Derivatives (1997)*.

[14] Stöcker, C., Zimmermann, M., & Christ, H. (2011). Effect of precipitation condition, prestrain and temperature on the fatigue behaviour of wrought nickel-based superalloys in the VHCF range. *Acta Materialia,59*(13), 5288-5304.

[15] Masuo, H., Tanaka, Y., Morokoshi, S., Yagura, H., Uchida, T., Yamamoto, Y., & Murakami, Y. (2018). Influence of defects, surface roughness and HIP on the fatigue strength of Ti-6Al-4V manufactured by additive manufacturing. *International Journal of Fatigue,117*, 163-179.

[16] Yamashita, Y., Murakami, T., Mihara, R., Okada, M., & Murakami, Y. (2017). Defect Analysis and Fatigue Design Basis for Ni-based Superalloy 718 manufactured by Additive Manufacturing. *Procedia Structural Integrity,7*, 11-18.

[17] AMS Standard 5562N, 1995 “Nickel Alloy, Corrosion and Heat Resistant, Bars, Forgings, and Rings 52.5Ni 19Cr 3.0Mo 5.1Cb 0.90Ti 0.50AI18Fe, Consumable Electrode or Vacuum Induction Melted 1775CF(968GC)Solution Heat Treated, Precipitation Hardenable,” AMS International, Materials Park, Ohio

[18] Retrieved from https://www.ssi.shimadzu.com/products/fatigue-testing/usf-2000a.html